

1 **Use of an Unmanned Aircraft System to Quantify NO_x Emissions**
2 **from a Natural Gas Boiler**

4 Brian Gullett¹, Johanna Aurell², William Mitchell¹, Jennifer Richardson³

5
6 ¹US Environmental Protection Agency, Office of Research and Development, Research Triangle Park, North
7 Carolina, 27711, USA; ²University of Dayton Research Institute, Dayton, Ohio, 45469-7532, USA; ³The Dow
8 Chemical Company, Midland, Michigan, 48667, USA.

9 *Correspondence to:* Brian Gullett (gullett.brian@epa.gov)

10
11 **Abstract**

12 Aerial emission sampling of four natural gas boiler stack plumes was conducted using an unmanned aerial system
13 (UAS) equipped with a light-weight sensor/sampling system (the “Kolibri”) for measurement of nitrogen oxide
14 (NO), and nitrogen dioxide (NO₂), carbon dioxide (CO₂), and carbon monoxide (CO). Flights (n = 22) ranged from
15 11 to 24 minutes duration at two different sites. The UAS was maneuvered into the plumes with the aid of real-time
16 CO₂ telemetry to the ground operators and, at one location, a second UAS equipped with an infrared/visible camera.
17 Concentrations were collected and recorded at 1 Hz. The maximum CO₂, CO, NO, and NO₂ concentrations in the
18 plume measured were 10,000 ppm, 7 ppm, 27 ppm, and 1.5 ppm, respectively. Comparison of the NO_x emissions
19 between the stack continuous emission monitoring systems and the UAS/Kolibri for three boiler sets showed an
20 average of 5.6 % and 3.5 % relative percent difference for the run-weighted and carbon-weighted average emissions,
21 respectively. To our knowledge, this is the first evidence for the accuracy performance of UAS-based emission
22 factors against a source of known strength.

23 Keywords: Emissions, natural gas, boiler, unmanned aircraft system, drone, continuous emission monitoring



26 **1 Introduction**

27 Aerial measurement of plume concentrations is a new field made possible by advances in Unmanned Aircraft
28 Systems (UAS, or “drones”), miniature sensors, computers, and small batteries. The use of a UAS platform for
29 environmental sampling has significant advantages in many scenarios in which access to environmental samples are
30 limited by location or accessibility. Hazards to equipment and personnel can also be minimized by the mobility of
31 the UAS as well as their ability to be remotely operated away from hazardous sources. UAS-based emission
32 samplers have been used for measurement of area source gases (Neumann et al., 2013; Rosser et al., 2015; Chang et
33 al., 2016; Li et al., 2018), point source gases (Villa et al., 2016), aerosols (Brady et al., 2016), black carbon particles
34 (Craft, 2014), volcanic pollutants (Mori et al., 2016), particle mass (Peng et al., 2015), and particle number
35 concentrations (Villa et al., 2016).

36 UAS-based emission measurements are particularly suited for area source measurements of fires and can be used to
37 determine emission factors, or the mass amount of a pollutant per unit of source operation, such as mass of
38 particulate matter (PM) per mass of fuel (e.g., biomass) burned. These values can be converted into emission rates,
39 such as mass of pollutant per unit of energy (e.g., g NO_x kJ⁻¹). These determinations typically rely on the carbon
40 balance method in which the target pollutant is co-sampled with the major carbon species present and, with
41 knowledge of the source’s fuel (carbon) composition, the pollutant to fuel ratio or an emission rate/factor, can be
42 calculated.

43 For internal combustion sources that have a process emission stack, downwind plume sampling can use the same
44 method. When combined with the source fuel supply rate and stack flow rates (to determine the dilution rate),
45 measurements comparable to extractive stack sampling may be possible. To our knowledge, determination of
46 emission factors from a stack plume using a UAS-borne sampling system has not previously been demonstrated. The
47 goal of this effort was to compare NO_x measurements obtained by UAS-borne emission samplers with those from
48 concurrent CEM measurements.

49 The feasibility of downwind plume sampling using a sensor-equipped UAS was tested on industrial boilers at the
50 Dow Chemical Company (Dow) facilities in Midland, Michigan (MI) and St. Charles, Louisiana (LA). The sensor
51 system was designed and built by the EPA’s Office of Research and Development and the UAS was owned and
52 flown by the Dow Corporate Aviation Group. To determine the comparative accuracy of the measurements, the
53 UAS-based emission factor was compared with the stack continuous emission monitoring systems (CEMS). The
54 target pollutants were nitrogen oxide (NO) and nitrogen dioxide (NO₂) to mimic the stack CEMS measurement
55 methods. Carbon as carbon dioxide (CO₂) and carbon monoxide (CO) were measured on the UAS for the carbon
56 balance method.

57 **2 Materials and Method**

58 Plume sampling tests were conducted on two natural-gas-fired industrial boilers located at Dow’s Midland,
59 Michigan and St. Charles, Louisiana facilities. The Midland boilers are firetube type boilers using low pressure
60 utility supplied natural gas. They are equipped with low NO_x burners and utilize flue gas recirculation to reduce
61 stack NO_x concentrations. The Midland facility burned natural gas with a higher heating value (HHV) of 9,697 kcal
62 m⁻³ (1089 British Thermal Unit (BTU)/ft⁻³). The two tested stacks are 14 m above ground level and 7 m apart. To
63 avoid sampling overlapping plumes, only a single boiler was operating during the testing. The St. Charles boilers are
64 D-type water package boilers using natural gas fuels (high pressure fuel gas (HPFG) and low pressure off-gas
65 (LPOG)). They are equipped with low NO_x burners with flue gas recirculation to reduce stack NO_x concentrations.
66 The boiler stacks are about 20 m apart and reach over 20 m in height above ground level. The St. Charles facility
67 burned natural gas under steady state conditions with a composition of 77.12 % CH₄, 2.01 % C₂H₆, and 19.91 % H₂

68 and a HHV of 7,845 kcal m⁻³ (881 BTU ft⁻³). Both boilers were operational during aerial sampling, but the wind
69 direction and UAS proximity to the target stack precluded co-mingling of the plumes.

70 Air sampling was accomplished with an EPA/ORD-developed sensor/sampler system termed the “Kolibri”. The
71 Kolibri consists of real-time gas sensors and pump samplers to characterize a broad range of gaseous and particle
72 pollutants. This self-powered system has a transceiver for data transmission and pump control (Xbee S3B, Digi
73 International, Inc., Minnetonka, MN, USA) from the ground-based operator. For this application, gas concentrations
74 were measured using electrochemical cells for CO, NO, and NO₂ and a non-dispersive infrared (NDIR) cell for CO₂
75 (Table 1). All sensors were selected for their applicability to the anticipated operating conditions of concentration
76 level and temperature as well as for their ability to rapidly respond to changing plume concentrations due to
77 turbulence and entrainment of ambient air. Each sensor underwent extensive laboratory testing to verify
78 performance and suitability prior to selection for the Kolibri. Tests included sensor performance (linearity, drift,
79 response time, noise, detection limits) in response to anticipated field temperatures, pressure, humidity, and
80 interferences. Additional information from the manufacturers on sensor performance is available from the links in
81 Table 1. In anticipation of temperatures as low as 0°C at the Midland site and to avoid daily temperature
82 fluctuations, insulation was added to the Kolibri frame and the sampled gases were preheated prior to the sensor
83 with the use of a heating element and micro fan inside the Kolibri. All sensors were calibrated before each sampling
84 day under local ambient conditions. After sampling was completed, the sensors were similarly tested to assess
85 potential drift.

86 Concentration data were stored by the Kolibri using a Teensy USB-based microcontroller board (Teensy 3.2, PJRC,
87 LLC., Sherwood, OR, USA) with an Arduino-generated data program and SD data card. All four sensors underwent
88 pre- and post-sampling two- or three-point calibration using gases (Calgasdirect Inc., Huntington Beach, CA, USA)
89 traceable to National Institute of Standards and Technology (NIST) standards.

90
91
92 **Table 1. UAS/Kolibri Target Analytes and Methods**

Analyte	Instrument, Manufacturer's Data Link	Frequency	Cal. Gases (ppm) Midland	Cal Gases (ppm) St. Charles
CO ₂	SenseAir CO ₂ Engine K30, NDIR ^a https://www.co2meter.com/products/k-30-co2-sensor-module	Continuous, 1 Hz ^b	408, 990	392, 996, 5890
CO	E2v EC4-500-CO, Electrochemical cell https://www.sgxsensorstech.com/content/uploads/2014/07/EC4-500-CO1.pdf	Continuous, 1 Hz	0 ^c , 9.67, 50.6	0, 9.9, 51.8
NO	NO-D4, Electrochemical cell http://www.alphasense.com/WEB1213/wp-content/uploads/2013/10/NOD4.pdf	Continuous, 1 Hz	0, 2.1, 41.4	0, 2.1, 40.4
NO ₂	NO ₂ -D4, Electrochemical cell http://www.alphasense.com/WEB1213/wp-content/uploads/2020/09/NO2-D4.pdf	Continuous, 1 Hz	0, 2.1, 10.4	0, 1.9, 10.4

93 ^aNon-dispersive infrared. ^bHz – hertz. ^cZero (0) cal gas = air.

94
95 The NO sensor (NO-D4) is an electrochemical gas sensor (Alphasense, Essex, UK) which measures concentration
96 by changes in impedance. The sensor has a detection range of 0 to 100 ppm with resolution of < 0.1 RMS noise

97 (ppm equivalent) and linearity within ± 1.5 ppm error at full scale. The NO-D4 was tested to have a response time to
98 95 % of concentration ($T_{95\%}$) of 6.3 ± 0.52 seconds and a noise level of 0.027 ppm. The temperature and relative
99 humidity (RH) operating range is 0 to $+50$ °C and 15 to 90 % RH, respectively.

100 The NO₂ sensor (NO2-D4) is an electrochemical gas sensor (Alphasense, Essex, UK) which likewise measures by
101 impedance changes. It has a NO₂ detection range of 0-10 ppm with resolution of 0.1 RMS noise (ppm equivalent)
102 and linearity error of 0 to 0.6 ppm at full scale. Its $T_{95\%}$ was measured as 32.3 ± 3.8 seconds with a noise level of
103 0.015 ppm. The temperature and RH operating range is 0 to $+50$ °C and 15 to 90 % RH, respectively.

104 Laboratory calibration testing prior to field measurements on both the NO-D4 and NO2-D4 sensors outputs showed
105 their responses to be linearly proportional ($R^2 > 0.99$) over the range of 4- and 5-point calibration gas
106 concentrations. The response times of both sensors were derived using the maximum reference concentration of
107 47.81 ppm for NO and 10.46 ppm of NO₂. The times to reach 95% of the reference concentration, t_{95} , were 6.3 and
108 32.3 sec (RSD (8.2% and 11.8%), respectively, for the NO-D4 and NO2-D4 sensors. These response times are both
109 shorter than those measured simultaneously in the laboratory by a CEM (Ametek 9000^{RM}, Pittsburgh, PA, USA) at
110 37 and 50 sec, respectively, for NO and NO₂.

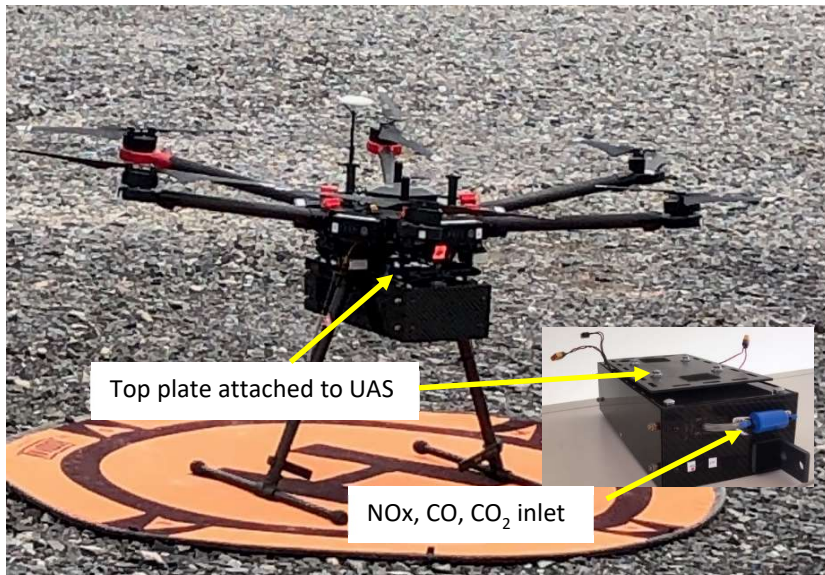
111 The CO₂ sensor (CO₂ Engine® K30 Fast Response, SenseAir, Delsbo, Sweden) is an NDIR gas sensor and the
112 voltage output is linear from 400 to 10,000 ppm. The temperature and RH operating range is 0 to $+50$ °C and 0 to 90
113 % RH, respectively. The CO₂-K30 sensor was measured to have a $t_{95\%}$ response time at 6000 ppm CO₂ of 9.0 ± 0.0
114 seconds and having a noise level of 1.6 ppm. The response time was 4 sec longer than compared to CO₂ measured
115 by a portable gas analyzer (LI-820, LI-COR Biosciences, Lincoln, NE, USA). The sensor and the LI-820 showed
116 good agreement as the measurements showed a R^2 of 0.99 and a slope of 1.01.

117 The CO sensor (e2V EC4-500-CO, SGX SensorTech Ltd, High Wycombe, Buckinghamshire UK) is described more
118 fully elsewhere (Aurell et al., 2017; Zhou et al., 2017). In previous sensor evaluation tests with laboratory biomass
119 burns (Zhou et al., 2017) with CO ranging between 0 and 250 ppm, the sensor was compared to simultaneous
120 measurements by a CO CEM (CAI Model 200, California Analytical Instruments Inc., Orange, CA, USA). The
121 concentration measurements had an $R^2 = 0.98$ and a slope of 1.04, indicating the level of agreement between the two
122 devices. The t_{90} was measured as 18 s while comparison of the time-integrated CO concentration differences with
123 the CAI-200, rated at $t_{90} < 1$ s, were only 4.9%.

124
125 Variations of the Kolibri sampling system allow for measurement of additional target pollutants. These include
126 particulate matter (PM), polycyclic aromatic hydrocarbons (PAHs), volatile organic compounds (VOCs) including
127 carbonyls, energetics, chlorinated organics, metals from filter analyses, and perchlorate (Aurell et al., 2017; Zhou et
128 al., 2017).

129 At both facilities the aviation team from Dow flew their DJI Matrice 600 UAS, a six-motor multicopter
130 (hexacopter), into the plumes with EPA/ORD's Kolibri sensor/sampler system attached to the undercarriage (Figure
131 1). In this configuration of sensors, the Kolibri system weighed 2.4 kg. Typical flight elevations at Midland and St.
132 Charles were 21 and 32 m above ground level (AGL), respectively, and flight durations ranged from 9 to 24 min.
133 At the St. Charles location, the UAS pilot was approximately 100 m from the center point of the two stacks, easily
134 allowing for line of sight operation. A telemetry system on the Kolibri provided real time CO₂ concentration and
135 temperature data to the Kolibri operator who in turn advised the pilot on the optimum UAS location.

136 CEMS on the boiler stacks produced a continuous record of NO_x emission and O₂ concentrations. Stack and CEMS
137 types located at the Midland and St. Charles facilities are shown in Table 2. The stack NO_x analyzer uses a
138 chemiluminescence measurement with a photomultiplier tube and is capable of split concentration range operation:
139 Low (0-180 ppm) and High (0-500 ppm). Its response time is reported as 5 sec. The O₂ analyzer uses a zirconium
140 oxide cell with a measurement range of 0 to 25% and a reported t_{95} of < 10 sec.



141 Figure 1. Dow UAS with Kolibri attached to the undercarriage.

142

143 **Table 2. CEMS Instruments at both Dow locations.**

Gas Measured	Midland CEMS	St. Charles CEMS
O ₂	Gaus Model 4705	ABB/Magnos 106
NO _x	Thermo Model 42i-HL	ABB/Limas 11

144

145 The plant CEMS undergo annual relative accuracy audit testing (NSPS Subpart Db, Part 70) using EPA Method 7E
 146 (2014) for NO_x and Method 3A (2017a) for O₂. Calculation of NO_x emissions use the appropriate F factor, a value
 147 that relates the required combustion gas volume to fuel energy input, as described in EPA Method 19 (2017b). Flue
 148 gas analysis for O₂ and CO₂ are performed in accordance with Method 3A (2017a) using an infrared analyzer to
 149 allow for calculation of the flue gas dry molecular weight.

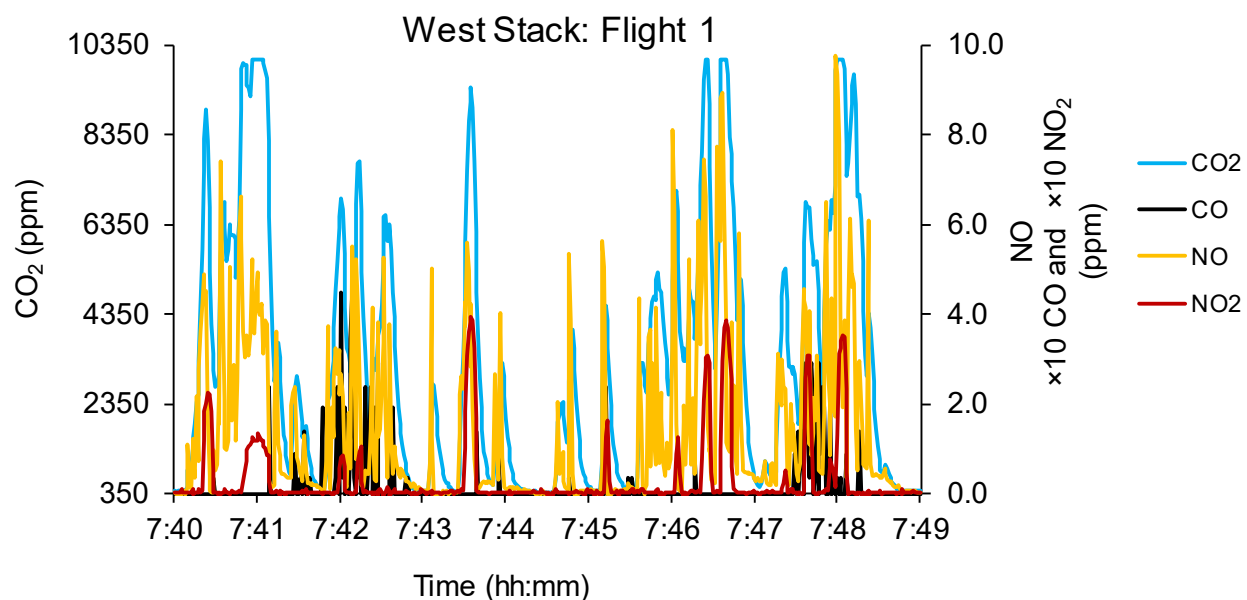
150 The CEMS and UAS/Kolibri data were reduced to a common basis for comparison of results. Emission factors, or
 151 mass of NO_x per mass of fuel carbon burned, and emission rates, or mass of NO_x per energy content of the fuel,
 152 were calculated from the sample results. The determination of emission factors, mass of pollutant per mass of fuel
 153 burned, depends upon foreknowledge of the fuel composition, specifically its carbon concentration, and its supply
 154 rate. The carbon in the fuel is presumed for calculation purposes to proceed to either CO₂ or CO, with the minor
 155 carbon mass in hydrocarbons and PM ignored for this source type. Concurrent emission measurements of pollutant
 156 mass and carbon mass (as CO₂ + CO) can be used to calculate total emissions of the pollutant from the fuel using its
 157 carbon concentration and fuel burn rate.

158 The UAS/Kolibri emission factors were calculated from the mass ratio of NO + NO₂ with the mass of CO + CO₂
 159 resulting in a value with units of mg NO_x kg⁻¹ C. CO₂ concentrations were corrected for upwind background
 160 concentrations. CEMS values of O₂ and fuel flowrate were used to calculate stack flowrate using US EPA Method
 161 19 (2017b). This Method requires the fuel higher heating value and an F factor (gas volume per fuel energy content,
 162 e.g., m³ kcal⁻¹ (ft³ BTU⁻¹)) to complete this calculation. For natural gas, the F factor is 967 m³ 10⁻⁶ kcal (8,710 ft³ 10⁻⁶

163 ⁶ BTU) (Table 19-2, EPA Method 19 (2017b)). The concentration, stack flowrate, and fuel flowrate data allow
164 determination of NO_x and C emission rates.

165 **3 Results and Discussion**

166 The UAS/Kolibri team easily found the stack plumes at both locations using the wind direction and CO₂ telemetry
167 data transmitted to the ground operator. Use of an infra-red (IR)/visible camera on a second UAS at St. Charles for
168 some of the flights aided more rapid location of the plume and positioning of the UAS/Kolibri. Gas concentration
169 fluctuations were rapid and of high magnitude as observed in a representative trace in Figure 2. CO₂ concentrations
170 to 10,000 ppm were observed; the relatively lower average CO₂ concentrations reflect the rapid mixing and
171 entrainment of ambient air causing dilution.



172
173 **Figure 2. Example of UAS/Kolibri-measured plume concentrations from the St. Charles West Boiler. Data**
174 **reported at 1 Hz.**

175 Sampling data and emission factors from the UAS/Kolibri are shown in Tables 3, 4, and 5 for the Midland, St.
176 Charles east stack, and St. Charles west stack, respectively. Eight sampling flights were conducted at the Midland
177 site, five on the St. Charles East boiler, and nine on the St. Charles West boiler. Both boilers at the Midland site
178 were operated under the same conditions, so their results have been presented together. Flight times averaged 14 min
179 (10 % relative standard deviation (RSD)) at the Midland facility and just over 20 min (10 % RSD) at the St. Charles
180 facility. The shorter flight times in Midland were due to lower UAS battery capacity caused by colder temperatures
181 (the sampling temperatures in the plume averaged 10±3°C). The average, multi-concentration drift for each of the
182 sensors, tested at both locations after each sampling day, was less than ±3%. The NO₂-D4 sensor showed higher
183 drift (average 8.6%) at one location for the highest concentration of its calibration gas (10.4 ppm). This had minimal
184 effect on the emission factor calibrations as the measured NO₂ in the plume was actually less than 1 ppm, a range
185 where the drift was much lower, and NO₂ is a minor contributor to the measured NO_x species.

186 Average plume NO_x concentrations were 0.88±0.32 ppm at Midland and 1.22 ppm and 2.41 ppm at the two St.
187 Charles boilers with an average RSD of 37 %, 36 %, and 12 %, respectively. The NO emission factor was typically
188 97 % of the total NO_x, with the NO₂ providing the minor balance.

189

190 **Table 3. Midland UAS/Kolibri Sampling Data and Emission Factors.**

Date	Flight	Flight time (hh:mm:ss)			NO ₂	NO	NO _x	Avg. CO ₂ ppm
		#	Up	Down	Total	mg kg ⁻¹ C	mg kg ⁻¹ C	
11/14/2018	1	10:29:00	10:43:00	00:14:00	201	618	819	1213
11/14/2018	2	11:13:04	11:28:28	00:15:24	186	624	810	1138
11/14/2018	3	12:54:17	13:08:47	00:14:30	230	659	889	2948
11/14/2018	5	13:27:40	13:42:05	00:14:25	99	570	669	4658
11/15/2018	6	10:24:20	10:39:30	00:15:10	61	394	454	3703
11/15/2018	7	10:41:36	10:52:40	00:11:04	84	397	481	3983
11/15/2018	8	10:55:10	11:10:10	00:15:00	126	398	524	4781
Average				00:14:13	141	523	664	3203
Stand. Dev.				00:01:28	65	121	179	1514
RSD (%)				10	46	23	27	47

191 Flight # 4 excluded from calculations as CO was observed, which originated from a cycling second boiler.

192

193 **Table 4. St. Charles East Stack UAS/Kolibri Sampling Data and Emission Factors.**

Date	Flight	Flight time (hh:mm:ss)			NO ₂	NO	NO _x	Avg. CO ₂ ppm
		#	Up	Down	Total	mg kg ⁻¹ C	mg kg ⁻¹ C	
07/23/2019	1	09:49:00	10:07:00	00:18:00	1	1442	1442	2305
07/23/2019	2	10:12:00	10:34:00	00:22:00	15	1461	1476	2526
07/23/2019	3	10:45:00	11:08:00	00:23:00	5	1534	1539	785
07/23/2019	4	11:11:00	11:31:00	00:20:00	101	1684	1785	1082
07/23/2019	5	11:52:00	12:01:00	00:09:00	107	2110	2217	1923
Average				00:20:45	30	1530	1560	1675
Stand. Dev.				00:02:13	47	110	155	869
RSD (%)				11	155	7.2	9.9	52

194 Flight # 5 was not included in the average as elevated CO concentrations were detected, likely from other sources
195 in the facility.

196

Date	Flight	Flight time (hh:mm:ss)			NO ₂	NO	NO _x	Avg. CO ₂ ppm
		#	Up	Down	Total	mg/kg C	mg/kg C	
07/24/2019	1	07:31:00	07:49:00	00:18:00	25	1366	1391	3221
07/24/2019	2	07:52:00	08:16:00	00:24:00	49	1263	1312	3503
07/24/2019	3	08:19:00	08:38:00	00:19:00	87	1420	1507	3415
07/24/2019	4	09:23:00	09:46:00	00:23:00	65	1341	1406	4509
07/24/2019	5	09:49:00	10:11:00	00:22:00	47	1296	1343	4813

07/24/2019	6	10:16:00	10:36:00	00:20:00	52	1299	1351	3773
07/24/2019	7	10:38:00	11:00:00	00:22:00	53	1316	1369	4194
07/24/2019	8	11:51:00	12:13:00	00:22:00	90	1460	1549	3129
07/24/2019	9	13:17:00	13:39:00	00:22:00	47	1464	1511	3606
Average				00:21:20	57	1358	1416	3796
Stand. Dev.				00:01:56	21	74	86	586
RSD (%)				9	36	5.5	6.0	15

197

198 Table 6 presents the average O₂ and NO_x measurement results and the fuel supply rate at both locations. Values for
 199 natural gas supply, adjusted for the C₂H₆ and H₂ composition of the St. Charles fuel, were used to calculate the fuel
 200 carbon supply rate. These data allow calculation of the emission factor, mass of NO_x to the mass of carbon, reported
 201 in Table 6.

202

203 **Table 5. Multi-Run Average Stack CEMS Data**

	Midland	St. Charles	
	Both Boilers	East Boiler	West Boiler
O ₂ (%)	8.2	4.9	4.5
NO _x (ppm)	15.7	50.4	42.9
Fuel rate	39.3 10 ⁶ kJ h ⁻¹	155.2 10 ⁶ kJ h ⁻¹	177.8 10 ⁶ kJ h ⁻¹

204

205 **Table 6. Comparison of Average NO_x Emission Factors from CEMS and UAS/Kolibri**

Run-Averaged NO _x Emission Factor, mg NO _x kg ⁻¹ C (\pm 1 std dev)			
	Midland	St. Charles	
	Both Boilers	East Boiler	West Boiler
CEMS	612 \pm 10	1555 \pm 50	1303 \pm 29
UAS/Kolibri	664 \pm 179	1560 \pm 155	1416 \pm 86
RPD: CEM & UAS/Kolibri, %	8.2	0.3	8.3

206

207 The UAS/Kolibri NO_x emission factor for Midland is 8 % higher than the simultaneous CEMS value. For the East
 208 and West boilers at St. Charles, the UAS/Kolibri NO_x emission factor value is <1 % and 8 % higher, respectively,
 209 than the CEMS values. The difference for the UAS/Kolibri in Midland may be attributed in part to the extremely
 210 cold temperature affecting the performance of the electrochemical sensors. The standard deviations for the CEMS
 211 data are based on the run-average NO_x values for each test. These values were calculated based on 10 sec averaging
 212 for the Midland tests, 60 sec averaging in St. Charles, and 1 sec averaging for the UAS/Kolibri. Higher standard
 213 deviations for the UAS/Kolibri are predictable given the rapidly changing values and wide range (~0-10 ppm) of
 214 NO_x data observed in Figure 2. Difference testing for the CEMS and UAS/Kolibri using α = 0.05 and assumed
 215 unequal variances indicate that only the West Boiler and UAS/Kolibri are statistically distinct.

216 The emission rates calculated from the UAS/Kolibri data are $5.6 \text{ kg NO}_x \cdot 10^{-3} \text{ kJ}$, $14.6 \text{ kg NO}_x \cdot 10^{-3} \text{ kJ}$, and 13.3 kg
217 $\text{NO}_x \cdot 10^{-3} \text{ kJ}$ (0.013, 0.034, and 0.031 lbs $\text{NO}_x \cdot 10^{-6} \text{ BTU}$), respectively, for the Midland, East St. Charles, and West
218 St. Charles boilers, below the regulatory standard of $15.5 \text{ kg NO}_x \cdot 10^{-3} \text{ kJ}$ (0.036 lbs $\text{NO}_x \cdot 10^{-6} \text{ BTU}$). The emission
219 factors were also calculated as carbon-weighted values to reflect potential differences in plume sampling efficiency
220 between runs. The Midland, East St. Charles, and West St. Charles UAS/Kolibri emission factors were, respectively,
221 607, 1525, and 1409 mg $\text{NO}_x \text{ kg}^{-1} \text{ C}$. These amounted to relative percent differences of 0.8, 1.9, and 7.8 % between
222 the CEM and UAS/Kolibri values, for an overall run-weighted average difference of 5.6 %. The difference between
223 the CEM readings and those from the Kolibri weighted by the carbon collection amounts, reflecting the success at
224 being within the higher plume concentrations, was 3.5 %.

225 **4 Conclusions**

226 This work reports, to our knowledge, the first known comparison of continuous emission monitoring measurements
227 made in a stack with downwind plume measurements made using a UAS equipped with emission sensors.

228 The UAS/Kolibri system was easily able to find and take measurements from the downwind plume of a natural gas
229 boiler despite lack of any visible plume signature. The telemetry system aboard the Kolibri system reported real time
230 CO_2 concentrations to the operator on the ground, allowing the operator to provide immediate feedback to the UAS
231 pilot on plume location. Comparison of the CEM data with the UAS/Kolibri data from field measurements at two
232 locations showed agreement of NO_x emission factors within 5.6 % and 3.5 % for time-weighted and carbon-
233 collection-weighted measurements, respectively.

234

235 Data availability. The tabular and figure data are available at the Environmental Dataset Gateway
236 <https://edg.epa.gov/metadata/catalog/main/home.page>.

237

238 Author contributions. BG was the prime author of the paper and the project lead. JA conducted the Kolibri field
239 testing and data analysis. WM designed the instrument electronics. JR led the UAS group and field test
240 arrangements.

241

242 Competing interests. The authors declare that they have no conflict of interest.

243

244 Disclaimer. The views expressed in this article are those of the authors and do not necessarily represent the views or
245 policies of the U.S. EPA.

246

247 Acknowledgements. Dow's Corporate Aviation Group: Laine Miller, Bryce Young, James Waddell, Jeffrey
248 Matthews, Chris Simmons, and Anthony DiBiase conducted flights flawlessly. Dow employees Rob Seibert and
249 Alex Kidd provided technical data and Amy Meskill (Dow), Jennifer DeMelo (Dow), and Dale Greenwell
250 (EPA/ORD) provided critical logistic support. Patrick Clark (Montrose) reviewed the St. Charles CEMS data.

251

252 Financial support. This work was supported through a Cooperative Research and Development Agreement between
253 the U.S. EPA and The Dow Chemical Company.

254

255

256

257 **References**

258 Aurell, J., W. Mitchell, V. Chirayath, J. Jonsson, D. Tabor, and B. Gullett. 2017. Field determination of
259 multipollutant, open area combustion source emission factors with a hexacopter unmanned aerial vehicle.
260 *Atmospheric Environment* **166**:433-440.

261 Brady, J. M., M. D. Stokes, J. Bonnardel, and T. H. Bertram. 2016. Characterization of a Quadrotor Unmanned
262 Aircraft System for Aerosol-Particle-Concentration Measurements. *Environmental Science & Technology*
263 **50**:1376-1383.

264 Chang, C.-C., J.-L. Wang, C.-Y. Chang, M.-C. Liang, and M.-R. Lin. 2016. Development of a multicopter-carried
265 whole air sampling apparatus and its applications in environmental studies. *Chemosphere* **144**:484-492.

266 Craft, T. L. C., C.F.; Walker, G.W. 2014. Using an Unmanned Aircraft to Observe Black Carbon Aerosols During a
267 Prescribed Fire at the RxCADRE Campaign. 2014 International Conference on Unmanned Aircraft
268 Systems **May 27-30, 2014**.

269 Li, X. B., D. F. Wang, Q. C. Lu, Z. R. Peng, Q. Y. Fu, X. M. Hu, J. T. Huo, G. L. Xiu, B. Li, C. Li, D. S. Wang, and
270 H. Y. Wang. 2018. Three-dimensional analysis of ozone and PM2.5 distributions obtained by observations
271 of tethered balloon and unmanned aerial vehicle in Shanghai, China. *Stochastic Environmental Research
272 and Risk Assessment* **32**:1189-1203.

273 Mori, T., T. Hashimoto, A. Terada, M. Yoshimoto, R. Kazahaya, H. Shinohara, and R. Tanaka. 2016. Volcanic
274 plume measurements using a UAV for the 2014 Mt. Ontake eruption. *Earth Planets and Space* **68**:18.

275 Neumann, P. P., V. H. Bennetts, A. J. Lilienthal, M. Bartholmai, and J. H. Schiller. 2013. Gas source localization
276 with a micro-drone using bio-inspired and particle filter-based algorithms. *Advanced Robotics* **27**:725-738.

277 Peng, Z.-R., D. Wang, Z. Wang, Y. Gao, and S. Lu. 2015. A study of vertical distribution patterns of PM2.5
278 concentrations based on ambient monitoring with unmanned aerial vehicles: A case in Hangzhou, China.
279 *Atmospheric Environment* **123**:357-369.

280 Rosser, K., K. Pavay, N. FitzGerald, A. Fatiaki, D. Neumann, D. Carr, B. Hanlon, and J. Chahl. 2015. Autonomous
281 Chemical Vapour Detection by Micro UAV. *Remote Sensing* **7**:16865-16882.

282 U.S. EPA Method 7E. 2014. Determination of Nitrogen Oxides Emissions from Stationary Sources (Instrumental
283 Analyzer Procedure). <https://www.epa.gov/sites/production/files/2016-06/documents/method7e.pdf>
284 Accessed August 7, 2019

285 U.S. EPA Method 3A. 2017a. Determination of oxygen and carbon dioxide concentrations in emissions from
286 stationary sources (instrumental analyzer procedure). https://www.epa.gov/sites/production/files/2017-08/documents/method_3a.pdf Accessed February 12, 2019

288 U.S. EPA Method 19. 2017b. Determination of sulfur dioxide removal efficiency and particulate matter, sulfur
289 dioxide, and nitrogen oxide emission rates. https://www.epa.gov/sites/production/files/2017-08/documents/method_19.pdf Accessed December 6, 2018

291 Villa, T. F., F. Salimi, K. Morton, L. Morawska, and F. Gonzalez. 2016. Development and Validation of a UAV
292 Based System for Air Pollution Measurements. *Sensors* **16**.

293 Zhou, X., J. Aurell, W. Mitchell, D. Tabor, and B. Gullett. 2017. A small, lightweight multipollutant sensor system
294 for ground-mobile and aerial emission sampling from open area sources. *Atm. Env.* **154**:31-41.